J|A|C|S
COMMUNICATIONS

Published on Web 04/14/2007

Deciphering the Structural Transformations during Nickel Oxyhydroxide Electrode Operation

Montse Casas-Cabanas,[†] Jesús Canales-Vázquez,[†] Juan Rodríguez-Carvajal,[‡] and M. Rosa Palacín*,[†]

Institut de Ciència de Materials de Barcelona (CSIC), Campus UAB E-08193 Bellaterra, Catalonia, Spain, and Institut Max Von Laue-Paul Langevin, BP 156 Grenoble Cedex 9, F-38042 France

Received November 24, 2006; E-mail: rosa.palacin@icmab.es

Nickel-based batteries using nickel hydroxide as the active material in the positive electrode have been extensively used since the publication of the first patents by Jügner[1,2] (Ni/Cd) and Edison[3,4] (Ni/Fe) and still today represent an important part of the rechargeable battery market. Although different technologies have been developed using a range of negative electrode materials such as Ni/H_2 or Ni/MH, the positive electrode material remains unchanged, that is, layered brucite type β-$Ni(OH)_2$ in the discharged (reduced) state and β-NiOOH in the charged (oxidized) state.

β-$Ni(OH)_2$ has a well-defined crystal structure with a hexagonal unit cell ($a = 3.13$ Å, $c = 4.61$ Å, space group $P\bar{3}m1$), which comprises an ABAB oxygen stacking sequence that results in edge-sharing NiO_6 octahedra layers, with protons filling the interlayer tetrahedral voids.[5] However, the complete structural characterization of β-NiOOH has not been achieved to date owing to the poor diffraction pattern, although there is a general agreement considering that no major modifications take place in the brucite structure upon oxidation.[6,7] In other words, it is assumed that no changes occur in the nickel positive electrode active material under working conditions, with the exception of an irreversible microstructural transformation that produces a mosaic texture during the first oxidation of β-$Ni(OH)_2$ as proposed by Delahaye et al. from low-resolution transmission electron microscopy (TEM) studies.[8] This process involves the formation of several slightly misoriented (nano) domains within each crystallite caused by the relaxation of the microstrains due to the subtle changes in the Ni−Ni distances as a consequence of the extraction of half the hydrogen atoms from the hydroxide.

To confirm or dismiss previous beliefs considering that the structure of β-$Ni(OH)_2$ remains largely intact upon oxidation, we combined high-resolution transmission electron microscopy (HRTEM) with X-ray diffraction (XRD) and neutron powder diffraction (NPD) to get further insight into the structure of β-NiOOH. This phase was chemically prepared at room temperature from industrial commercial β-$Ni(OH)_2$ (Friwo GmbH) mimicking the processes occurring upon battery charge/discharge. The oxidation of pristine β-$Ni(OH)_2$ to yield β-NiOOH has been performed using dry ozone as the oxidizing agent to avoid impurities of the more oxidized phase γ-NiOOH often encountered in wet synthetic routes, which demand the use of both higher temperatures and solutions containing alkaline ions.[9] γ-NiOOH exhibits a more expanded structure that accommodates alkaline ions in the interlayer space and only appears in nickel batteries after prolonged overcharge. Mild chemical reduction of β-NiOOH carried out at room temperature using H_2O_2 (30% (w/v) in H_2O) produces β-$Ni(OH)_2$ (hereafter denoted as chemically cycled β-$Ni(OH)_2$), which has also been studied and characterized for comparison with pristine β-$Ni(OH)_2$).[8] All three samples have been investigated by HRTEM and their diffraction patterns refined with the Rietveld method using the FullProf program.[10,11] Realistic models considering the anisotropic broadening of the diffraction peaks in β-$Ni(OH)_2$ owing to both the very small platelet-shaped crystallites and the presence of microstrains were necessary to extract appropriate structural and microstructural information from the diffraction peak profiles.

The HRTEM images corresponding to the as-received β-$Ni(OH)_2$ used in this study (Figure 1) reveal hexagonal platelet-shaped particles with an average diameter of approximately 300 Å, in agreement with previous investigations in a range of laboratory and industrial β-$Ni(OH)_2$ samples.[12] Stacking faults along the *c*-axis can be observed, as extensively reported for battery grade β-$Ni(OH)_2$,[13−15] although the HRTEM images recorded along several other zone axes reveal highly crystalline particles free of defects. These observations fully agree with the corresponding Rietveld refinement, which has been performed considering the structural parameters reported by Greaves and Thomas from NPD data[5] as ab initio values and using spherical harmonics to model the anisotropic peak broadening due to size effects. The refined cell parameters are $a = 3.12889(9)$ Å and $c = 4.6554(4)$ Å, while the calculated average crystallite diameter and thickness are 346 and 109 Å, respectively. The data analysis also reveals the presence of microstrains along the 001 direction, which is consistent with the presence of stacking faults.

β-NiOOH tends to degrade inside electron microscope columns, which has hampered to date the success of HRTEM studies. Nevertheless, such limitations may be overcome by operating under low-beam irradiation conditions and short-term exposures. The recorded HRTEM images reveal that β-NiOOH particles exhibit a mosaic texture and consist of 5−10 nm domains with a large concentration of microstrains, which in turn result in slightly misoriented subdomains covering few unit cells. However, the most striking result of our study is the doubling of the *c*-axis in β-NiOOH compared to β-$Ni(OH)_2$, as shown in Figure 1. Despite the considerable degree of microstrains detected in the HRTEM images, this feature has been observed in all the β-NiOOH crystals investigated and is consistent with old reports describing a weak reflection observed at $d \approx 9.3$ Å in the corresponding XRD pattern[16] and, though it was regarded as compatible with a larger unit cell, was mostly assigned to impurities and not mentioned in any more recent studies. Consequently, the microstructure of β-NiOOH is far more complex than that of β-$Ni(OH)_2$, which strongly perturbs the long-range ordering and limits the information that can be extracted from the diffraction data. Assuming that the Ni−O bonds

[†] Institut de Ciència de Materials de Barcelona (CSIC).
[‡] Institut Max Von Laue-Paul Langevin.

10.1021/ja068433a CCC: $37.00

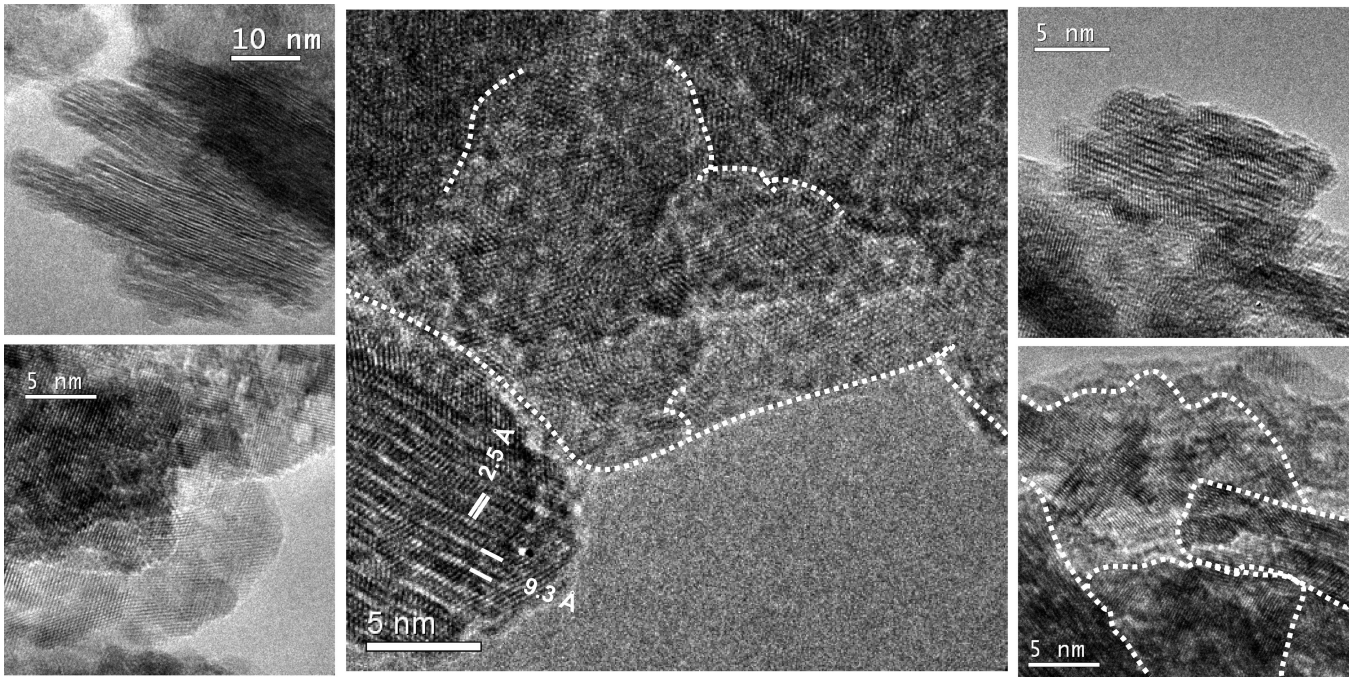

Figure 1. HRTEM images corresponding to pristine β-Ni(OH)$_2$, β-NiOOH, and chemically cycled β-Ni(OH)$_2$: pristine β-Ni(OH)$_2$ viewed (a) perpendicular to and (b) down the *c*-axis, revealing rather coherent and crystalline domains; (c) a typical image of different β-NiOOH particles where the *c*-axis is doubled upon oxidation and a mosaic strained microstructure appears; (d, e) images of chemically cycled β-Ni(OH)$_2$ exhibiting the original stacking sequence along the *c*-axis with retention of the mosaic texture.

in the NiO_6 layers do not break upon oxidation of β-Ni(OH)$_2$, ABCA is the only oxygen stacking sequence compatible with the observed doubling of the unit cell in β-NiOOH. The combined X-ray/neutron Rietveld refinement has thus been attempted considering an ABCA stacking structure with a range of models to account for anisotropy in microstrains and peak broadening owing to the crystallite size. The best results were obtained by treating the former with a limited development of spherical harmonics and the latter through the use of a quadratic form in reciprocal space considering ellipsoidal crystallite morphology. In the first stages of the refinement, the Ni−O distances were restrained to the values obtained from previous extended X-ray absorption fine structure (EXAFS) studies.[17] Hydrogen atoms were located by restraining the O−H distance to ca. 0.9 Å, and their occupations were refined in the last refinement stages and found to converge to the nominal value. The final refined cell parameters are $a = 4.883(5)$ Å, $b = 2.920(8)$ Å, $c = 9.24(1)$ Å, and $\beta = 88.8(1)°$ ($C2/m$ space group, see Supporting Information). The microstructural information extracted from the diffraction line profile is again in very good agreement with HRTEM observations, as the resulting amount of microstrains is much higher than in the case of pristine β-Ni(OH)$_2$, especially in the *ab* plane. Moreover, the average crystallite basal dimensions (43 and 132 Å axes) and thickness of 85 Å are consistent with the formation of the mosaic texture also detected in the HRTEM images. A plot of the experimental and calculated diffraction patterns is shown in Figure 2, and the resulting average crystal structure is shown in Figure 3.

These results indicate that layer shearing perpendicular to the *c* direction occurs during the oxidation of β-Ni(OH)$_2$, as is well-known for the oxidation of related phases such as β-Co(OH)$_2$.[18,19] This is in agreement with the first principles calculations published in the course of our investigations,[20] which point out that the β-Ni(OH)$_2$ layer stacking is not thermodynamically favored as hydrogen atoms are withdrawn. One should note that the ABCA layer sequence proposed for β-NiOOH can be regarded as a stacking fault in the ideal ABAB arrangement of β-Ni(OH)$_2$, and thus it is

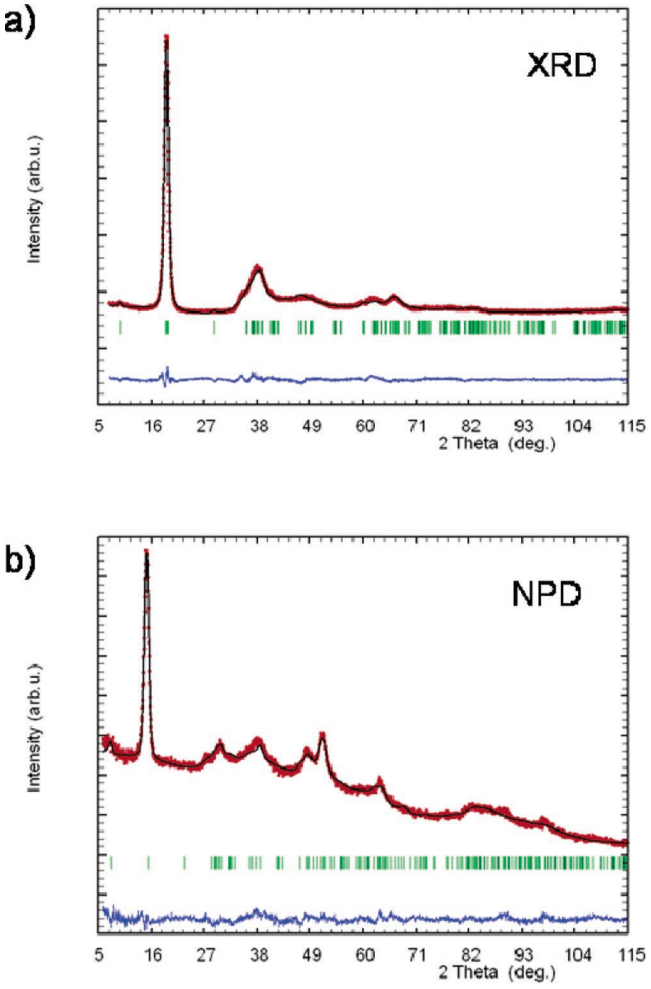

Figure 2. (a) X-ray and (b) neutron powder diffraction patterns (small circles) showing the final Rietveld fit (solid line), with the difference pattern below.

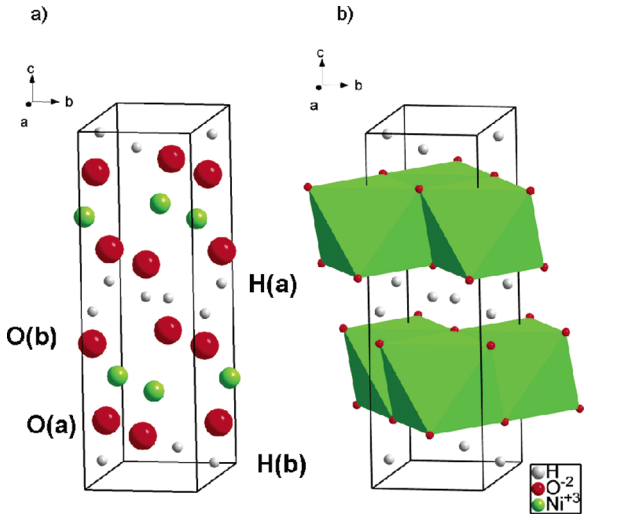

Figure 3. β-NiOOH unit cell: (a) atomic and (b) polyhedral representations.

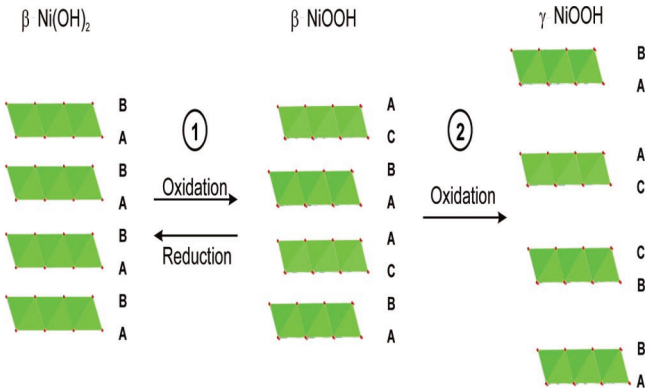

Figure 4. Schematic representations corresponding to the structural transformations occurring in the positive electrode upon nickel battery standard operation (1) and overcharge (2).

very likely to already exist locally in the structure of β-Ni(OH)$_2$. Furthermore, the ABCA ordering of β-NiOOH can also be considered as an intermediate stage in the transformation from ABAB to the ABBCCA oxygen stacking sequence of γ-NiOOH, which in turn may appear in battery electrodes upon over-oxidation, as already mentioned above (see Figure 4).

The HTREM investigations on chemically cycled β-Ni(OH)$_2$ (Figure 1) indicate that, despite the fact that the mosaic texture is retained, the *d*-spacing corresponding to the *c*-axis is approximately 4.6 Å, hence confirming that the sheared structure reverts to the original layer stacking sequence after proton insertion during reduction. The Rietveld refinement may thus be achieved using the same structural and microstructural models considered for pristine β-Ni(OH)$_2$, with $a = 3.1253(9)$ Å and $c = 4.689(4)$ Å and microstrains affecting preferentially the 001 direction. The preservation of the mosaic texture is confirmed by the calculated average crystallite diameter and thickness (145 and 105 Å, respectively). These observations are in full agreement with the well-known reversibility of the redox process in this system.

In conclusion, we have been able to determine the crystal structure of β-NiOOH and hence demonstrate that reversible severe structural changes take place in nickel battery positive electrodes upon operation which enables us to understand the operation mechanism of nickel-based batteries at the atomic level. Critical to the success of this task was the simultaneous consideration of structural and microstructural models in the Rietveld refinement of both the reduced phase and the oxidized phase and the combination of two complementary techniques, that is, HRTEM and powder diffraction.

Acknowledgment. We are grateful to J. Oró-Solé, F. Bardé, and A. Van der Ven for valuable discussions and to J. Bassas for X-ray diffraction data acquisition.

Supporting Information Available: General experimental details, Rietveld refinement details, and structural information (PDF); crystallographic file for β-NiOOH (CIF). This material is available free of charge via the Internet at http://pubs.acs.org.

References

(1) Jugner, W. Verfahren zur Elektrolytischen Vergrösserung der Oberfläche von Masseträgern aus Eisen, Nickel oder Kobalt für Elektroden in alkalischen Sammlern. German Patent 163 170, 1901.
(2) Jugner, W. Elektrischen Sammlern mit unveränderlichem alkalischen Elektrolyten. German Patent 157 290, 1901.
(3) Edison, T. A. Reversible galvanic battery. U.S. Patent 678 722, 1901.
(4) Edison, T. A. Method of making electrodes. U.S. Patent 880 027, 1908.
(5) Greaves, C.; Thomas, M. A. *Acta Crystallogr., Sect. B: Struct. Sci.* **1986**, *42*, 51−55.
(6) Oliva, P.; Leonardi, J.; Laurent, J. F.; Delmas, C.; Braconnier, J. J.; Figlarz, M.; Fievet, F.; Guibert, A. de *J. Power Sources* **1982**, *8*, 229−255.
(7) McBreen, J. The nickel oxide electrode. In *Modern Aspects of Electrochemistry*; White, R. E., Bockris J. O'M., Conway, B. E., Eds.; Plenum Press: New York, 1990; pp 29−63.
(8) Delahaye-Vidal, A.; Beaudoin, B.; Figlarz, M. *React. Solid.* **1986**, *2*, 223−233.
(9) Bardé, F.; Palacín, M. R.; Beaudoin, B.; Tarascon, J. M. *Chem. Mater.* **2005**, *17*, 470−476.
(10) Rodríguez-Carvajal, J. *Physica B* **1993**, *192*, 55−69.
(11) For a more recent version see: Rodríguez-Carvajal, J. *CPD Newslett.* **2001**, *26*, 12. http://journals.iucr.org/iucr-top/comm/cpd/Newsletters/. (The program and documentation can be obtained from http://www.ill.fr/dif/Soft/fp.)
(12) Casas-Cabanas, M.; Rodríguez-Carvajal, J.; Canales-Vázquez, J.; Palacín, M. R. *J. Mater. Chem.* **2006**, *28*, 2925−2939.
(13) Wronski, Z. S.; Carpenter, G. J. C.; Kalal, P. J. Proceedings of the 190th ECS Meeting, San Antonio, TX, October 1996; Electrochemical Society: Pennington, NJ, 1996; pp 96−14, 177−188.
(14) Delmas, C.; Tessier, C. *J. Mater. Chem.* **1997**, *7*, 1439−1443.
(15) Tessier, C.; Haumesser, P. H.; Bernard, P.; Delmas, C. *J. Electrochem. Soc.* **1999**, *146*, 2059−2067.
(16) Bode, H.; Dehmelt, K.; Witte, J. *Z. Anorg. Chem.* **1969**, *366*, 1−21.
(17) Demourgues, A.; Gautier, L.; Chadwick, A. V.; Delmas, C. *Nucl. Instrum. Methods Phys. Res. B* **1997**, *133*, 39−44.
(18) Lotmar, W.; Feitknecht, W. *Z. Kristallogr. Krist.* **1936**, *93*, 368−378.
(19) Delaplane, R. G.; Ibers, J. A.; Ferraro, J. R.; Rush, J. J. *J. Chem. Phys.* **1969**, *50*, 1920−1927.
(20) Van der Ven, A.; Morgan, D.; Meng, Y. S.; Ceder, G. *J. Electrochem. Soc.* **2006**, *153*, A210−A215.

JA068433A